Journal of Food Engineering 339 (2023) 111282

Contents lists available at ScienceDirect

Journal of Food Engineering

journal homepage: www.elsevier.com/locate/jfoodeng

The effect of pine cone lignin on mechanical, thermal and barrier properties of faba bean protein films for packaging applications

Sandra Rojas-Lema [a], Klara Nilsson [b], Maud Langton [b], Jon Trifol [c,d,e], Jaume Gomez-Caturla [a], Rafael Balart [a], Daniel Garcia-Garcia [a,*], Rosana Moriana [b,c,f]

[a] Instituto de Tecnología de Materiales (ITM), Universitat Politècnica de València (UPV), Plaza Ferrándiz y Carbonell 1, 03801, Alcoy, Alicante, Spain
[b] Department of Molecular Sciences, Swedish University of Agricultural Sciences (SLU), Box 7051, SE-750 07, Uppsala, Sweden
[c] Department of Fibre and Polymer Technology, School of Engineering Sciences in Chemistry, Biotechnology and Health, Royal Institute of Technology (KTH), SE-100 44, Stockholm, Sweden
[d] Gaiker Technology Center, Basque Research and Technology Alliance (BRTA), Parque Tecnológico de Bizkaia, Edificio 202, 48170, Zamudio, Spain
[e] Department of Chemical and Metallurgical Engineering, School of Chemical Engineering, Aalto University, P.O. Box 16300, FIN-00076 Aalto, Espoo, Finland
[f] RISE Bioeconomy and Health, Research Institute of Sweden (RISE), Drottning Kristinas Väg 61, SE-114 28, Stockholm, Sweden

ARTICLE INFO

Keywords:
Proteins films
Faba beans
Pine cone
Lignin
Packaging

ABSTRACT

In the present work, faba bean protein (FBP) films plasticized with glycerol and reinforced with different amounts (2.5, 5.0, 7.5 and 10% by weight of FBP) of lignin extracted from pine cones (PL) have been obtained by solution casting. The results obtained showed an elongation at break of 111.7% with the addition of 5% PL to the FBP film, which represents an increase of 107% compared to the FBP control film. On the other hand, it was observed by thermogravimetric analysis (TGA) that the incorporation of lignin improved the thermal stability of the FBP film, leading to an increase in the protein degradation temperature, being this increase higher in the sample film reinforced with 10% PL. The barrier properties of the FBP films were also affected by the presence of lignin, leading to a decrease in water vapor permeability (WVP) in comparison to the unreinforced film. The results show that the sample reinforced with 2.5% PL had the lowest WVP value, with a reduction of 25% compared to the control film. Chemical analysis by Fourier transform infrared spectroscopy (FTIR) confirmed the formation of intramolecular interactions between lignin and proteins which, together with the inherent hydrophobicity of lignin, resulted in a decrease of the moisture content in the films reinforced with PL. This research work has allowed the development of biobased and biodegradable films with attractive properties that could be of potential use in sectors such as packaging.

1. Introduction

Currently, due to growing environmental and economic problems, lignocellulosic biomass, which is a renewable resource, constitutes a promising alternative to non-renewable petroleum resources. For instance, biopolymers obtained from natural sources offer a great opportunity since they have interesting properties, such as renewability and biodegradability (Sadasivuni et al., 2020; Yadav et al., 2018) and, in some cases, they can offer even biocompatibility (Gnanasekaran, 2019; Nagarajan et al., 2019). Therefore, they can be considered as environmentally friendly materials (Bourtoom, 2009).

An interesting application of biopolymers includes packaging that could replace single-use synthetic plastics that cause a great amount of waste (Denavi et al., 2009; Dey et al., 2021; Walker et al., 2021). That is one of the reasons why different sectors such as the food industry have focused on finding materials with biodegradable properties in order to find new packaging to protect and extend food shelf life (Montalvo-Paquini et al., 2014). A wide range of biopolymers can be found in nature, among them lipid-based polymers, proteins and polysaccharides including cellulose and starch, among others (Shankar et al., 2015), that represent promising options to be used as biobased and biodegradable materials. With regard to polysaccharides, they can provide different properties, including thickening, crosslinking, and adsorption (Xia et al., 2020). In the case of cellulose, it could provide high crystallinity to these biobased materials (Khalil et al., 2017). Starch offers excellent biocompatibility and exceptional film-forming properties (Agarwal,

* Corresponding author.
E-mail addresses: sanrole@epsa.upv.es (S. Rojas-Lema), dagarga4@epsa.upv.es (D. Garcia-Garcia).

https://doi.org/10.1016/j.jfoodeng.2022.111282
Received 7 May 2022; Received in revised form 25 July 2022; Accepted 7 September 2022
Available online 10 September 2022

2021). In the case of proteins, they have been used as films for packaging, especially because of their apparent good oxygen barrier properties, and unique structure that allow having good mechanical properties. This is caused by the existence of a high amount of polar groups in its structure, leading to high intermolecular binding (Anker et al., 2000). However, this property is still low compared with synthetic polymers (Bourtoom, 2009). Another drawback of protein films is their poor water vapor barrier due to their inherent hydrophilicity (González et al., 2011; Montalvo-Paquini et al., 2014). To overcome some of the limitations presented by proteins, different strategies have been investigated, including mixing with hydrophobic additives, *e.g.* fatty acids (Jongjareonrak et al., 2006; Niegelhell et al., 2017), lipids (Garcia et al., 2000; Rhim, 2004), waxes (Kim et al., 2002; Niegelhell et al., 2017), or simply changing the drying conditions (Denavi et al., 2009). Another of the studied methods include the use of cross-linkers such as formaldehyde (Rhim et al., 2000), glutaraldehyde (Marquié, 2001), and glyoxal (Makishi et al., 2013), among others. All these strategies try to enhance the cohesion properties of the protein polymeric matrix with the main objective of improving the barrier and mechanical properties (De Carvalho and Grosso, 2004). Nevertheless, some of them give somewhat cytotoxicity and are not suitable for use in food packaging (González et al., 2011). One of the most widely used alternatives to enhance the flexibility, extensibility and processability of proteins involves the use of plasticizers (Kokoszka et al., 2010; Ramos et al., 2013), being glycerol the most commonly used because it is biodegradable, non-toxic and recyclable properties (Pagliaro et al., 2007; Wolfson et al., 2007). Currently, the use of proteins combined with some other natural materials as biopolymers is being studied. Surprisingly, despite that lignin is the second most abundant natural polymer on the earth after cellulose, its use as additive in protein-based polymers has barely been investigated (Austin and Ballaré, 2010; Upton and Kasko, 2016). Lignin is an amorphous polymer that contains three phenylpropanolic monomers linked by carbon - carbon and ether bonds (Upton and Kasko, 2016). It has many reactive hydroxyls groups that are capable of forming strong hydrogen bonds with polymers, which could allow improving physical properties such as adhesion, adsorption, among others (Ciobanu et al., 2004; Liu et al., 2005). In addition, lignin is a low-cost raw material and it has been normally used as low-value fuel (Upton and Kasko, 2016). Therefore, it could be used to obtain lignin-based materials with higher added value. Lignin can be considered as a good reinforcement for proteins due to its intrinsic hydrophobicity that could contribute to improve moisture resistance to protein-based films (Gadhave et al., 2019). In addition, the hydrogen in the phenolic group of lignin can readily interact with some functional group in protein to give a cross-linked structure. This may contribute to the increase in tensile strength, thermal stability, and Young's modulus (Gadhave et al., 2019; Huang et al., 2003). There are some studies that report the use of lignin and its positive effects on protein-based films. Arancibia et al. (2014), obtained bilayer films with isolated soy protein isolated, lignin, and formaldehyde. The use of lignin provided a noticeable improvement in protection against UV-VIS light, which might happen due to the strong light absorption of lignin and its capacity for autoxidation. Gomide et al. (2021), reported the improvement in the thermal and mechanical properties in protein-based films of whey protein isolate with different amounts of lignin microparticles. Moreover, the films containing the highest amount of lignin microparticles of 0.75% (w/w) showed antioxidant properties. Zadeh et al. (2018) reported interesting properties of isolate soy protein films for packaging applications. They reported the use of lignin-based additives, namely lignosulfonate and alkali lignin. With regard to lignosulfonate, this allowed to improve mechanical properties and water absorption, meanwhile, films with alkali lignin offered high light absorption in the UV region.

Faba bean (*Vicia faba* L.), are considered to be one of the oldest grain-legume crops, and still has an important world production (Alharbi and Adhikari, 2020; Hendawey and Younes, 2013). They are a rich source of carbohydrates (51–68%, dry matter) and proteins (20–41%, dry matter). The growing conditions and the type of grain influence the proportion of protein and carbohydrate (Hendawey and Younes, 2013). Faba bean has been traditionally used in Mediterranean countries, as well as other countries as Pakistan, India, China among others. It has been also used as animal feed and to prevent soil erosion as a cover crop (Vioque et al., 2012), so the idea to use this high-protein content bean in other high added-value applications could be promising. Faba bean has been proposed as biobased polymer for films with potential uses in the food industry (Montalvo-Paquini et al., 2013; Saremnezhad et al., 2011)

The purpose of the present study is to analyze how the addition of different lignin contents derived from pine cone (2.5, 5.0, 7.5 and 10 wt %) influences the thermal, mechanical, morphological, barrier and optical properties of FBP films. Furthermore, the effect of lignin on the water susceptibility of the FBP film, as well as on its structural modifications, has also been studied. The authors expect lignin and faba bean protein to interact through hydrogen bonding, as both components possess hydroxyl functionalities that could react with each other and help to improve the linkage between them in the film.

2. Experimental

2.1. Materials

Faba beans of the *gloria variety* used were provided by the Research Institutes of Sweden (RISE). The lignin was obtained from pine cones of the *Pinus Pinea* species, collected in pine forests in the mountains of Alicante (Spain). Glycerol ($C_3H_8O_3$, purity $\geq$99.0%) was supplied from Sigma Aldrich (Madrid, Spain). Hydrochloric acid (HCl, purity of 36%) and sodium hydroxide (NaOH, purity >97.0%) were provided by VWR (Darmstadt, Germany).

2.2. Isolation of faba bean protein (FBP)

The isolation of bean protein (FBP) was performed according to the methodology reported by Rojas-Lema et al. and is widely used in protein isolation (Rojas-Lema et al., 2021). For this, faba bean were dehulled, and then milled in order to obtain a powdered flour. The milling process was carried out in a rotary mill from Brabender (Duisburg, Germany). Subsequently, faba bean flour was added to distilled water at a ratio 1:10 (w/v) and the pH of the obtained solution was adjusted to 9.0 using a 2 M NaOH solution to improve the protein solubility. The final solution was stirred at room temperature for 1 h, then it was centrifuged in a Sorvall Lynx 6000 centrifuge from Thermo Scientific (Langenselbold, Germany) at 3700 G for 30 min and 18 °C. The pH of supernatant was adjusted to 4.0 using a 1M HCl solution to precipitate the protein. It was stirred at room temperature for 1.5 h and centrifuged at 3700 G for 30 min and 18 °C. The precipitates were collected and re-dispersed in distilled water with a ratio 1:10 (w/v). The pH of the suspension was changed to 4.0 and then, centrifuged in the same conditions as above. Finally, the precipitated protein obtained was frozen and freeze-dried.

2.3. Isolation of pine cone lignin (PL)

The lignin was extracted from a side stream of a pine cone biorefinery process as described by Trifol et al. (2021) with minor modifications. Briefly, pine cone particles were treated with two consecutive alkali treatments, firstly at 1.5 M NaOH at 110 °C for 1 h and thereafter at 1M NaOH and 155 °C for 3 h. The mixture was separated by filtration and the liquor fraction obtained from the second alkali treatment was subjected to an acid precipitation in order to obtain the lignin. For this, the liquor was heated to 60 °C under magnetic stirring, and sulfuric acid (64 wt%) was added dropwise until reaching pH 2. The solution was kept for 30 min under magnetic stirring and cooled in an ice bath. Subsequently, the solution was centrifuged at 3000 rpm for 5 min to recover the sediment fraction. Finally, the sediment was frozen and freeze-dried to obtain the pine cone lignin (PL) used.

The obtained fraction showed a lignin content of 73%, the rest was 16% of hemicelluloses (mainly xylose and arabinose), 4% of cellulose and 6% of ashes. The average molecular weight (M_w) of lignin fraction was 11,740 g/mol with a polydispersity index (PDI; M_w/M_n) of 2.92 (Trifol et al., 2021).

2.4. Preparation of FBP/PL films

Faba bean protein films were prepared by a solution casting method. Control film was prepared dissolving 3% (w/v) of FBP in distilled water and then, adding 30% (w/w) of glycerol with respect to the dry weight of FBP. The resultant solution was adjusted to pH of 10.5 using a 2 N NaOH solution and kept under mechanical stirring for 1 h. Then, the resultant solution was heated in a water bath to 80 °C during 30 min, and then cooled down to room temperature in order to promote protein denaturation. FBP/PL films were prepared using the same process as for the control film but with the addition of different amounts of PL (2.5, 5, 7.5, and 10 wt% based on the dry weight of FBP) after 1 h of stirring. After lignin addition, the solution was adjusted to pH 10.5 and stirred by 2 h, and then denatured as indicated before. The different solutions prepared were placed into Petri dishes and dried for 24 h at 50 °C to remove water. The films were then conditioned in a desiccator at 25 °C and 50% relative humidity (RH) for 48 h before testing. All films were developed in triplicate. The film compositions can be observed in Table 1.

2.5. Characterization techniques

2.5.1. Film thickness

A micrometer from Kalkum Ezquerra (La Rioja, Spain) with a sensitivity of ±0.001 mm was used to measure the thickness of the films. All films were measured on at least ten random points in different parts of the film, and the average value was determined.

2.5.2. Thermal properties

The thermal stability of the FBP/PL films was examined in triplicate by thermogravimetry (TGA) on a thermogravimetric balance Linseis model PT1000 (Selb, Germany). The samples, weighing about 13–15 mg, were placed in 70-μL standard alumina crucibles and subjected to a heating program from 30 °C to 700 °C at a heating rate of 10 °C/min in nitrogen atmosphere (with a constant flow rate of 66 mL/min).

2.5.3. Mechanical properties

Tensile tests of the films were carried out in a universal test machine Elib 50 from S.A.E. Ibertest (Madrid, Spain), following the standard method ISO 527–3:2018. Tests were performed using a load cell of 100 N and a cross-head speed of 5 mm/min at room temperature. Rectangular samples (6 × 80 mm^2) of each film were placed between the clamps with an initial gap of 50 mm. Five samples of each composition were tested and the corresponding tensile strength, Young's modulus and elongation at break were averaged.

2.5.4. Moisture content

The moisture content (MC) of FBP control film and FBP/PL films was determined gravimetrically through the weight loss measurement of the films, following the procedure described by González et al. (2019). For this end, preconditioned samples (1 × 1 cm^2) were weighed. Then they were dried for 24 h in an oven at 105 °C and weighed again. The MC of each film was obtained in triplicate following Equation (1).

$$MC(\%) = \left[\frac{Initial\ film\ weight\ -\ Dried\ film\ weight}{Initial\ film\ weight}\right] \times 100 \quad (1)$$

2.5.5. Water solubility

The water solubility (WS) of FBP control film and its composites with PL was obtained triplicate following the method described by Masamba et al. (2016), with few modifications. For this, the different films were cut into square pieces (1 × 1 cm^2), dried for 24 h in an oven at 105 °C and subsequently weighed. The films were then deposited into a tube with 10 mL of distilled water during 24 h at room temperature. The undissolved films were then dried in an oven at 105 °C for 24 h and finally weighed. The water solubility of films was determined by following Equation (2):

$$WS\ (\%) = \left[\frac{Initial\ film\ weight\ -\ Dried\ film\ weight}{Initial\ film\ weight}\right] \times 100 \quad (2)$$

2.5.6. Static contact angle

The film surface wettability was studied through the water contact angle (θ) measurement using an optical goniometer EasyDrop-FM140 from Kruss Equipment (Hamburg, Germany) following the ISO 828:2013. In this case, a drop of distilled water (5 μL) was deposited on the film surface exposed to air during the drying process and the angle between the droplet and the film surface was determined using an image analyzer software. All the contact angles measurements were carried out at 15 s after the droplet was deposited on the film surface. For each film, ten measurements of the water contact angle were collected and averaged.

2.5.7. Color parameters

Color of the FBP control film and its composites with PL was determined with a KONICA CM-3600d COLORFLEX-DIFF2 colorimeter, from Hunter Associates Laboratory (Virginia, USA). The colorimeter was calibrated using a standard white tile and the measurements were obtained using standard illuminant D65 and an observer angle of 10°. L^*, a^*, and b^* color coordinates were measured on each film. Five different measurements were taken and the corresponding color coordinates were averaged. The total color difference (ΔE) was determined by Equation (3):

$$\Delta E = \sqrt{(\Delta L^*)^2 + (\Delta a^*)^2 + (\Delta b^*)^2} \quad (3)$$

where ΔL^*, Δa^* and Δb^* are the color parameters differences between samples and the control film ($L^* = 40.9$, $a^* = 1.7$, $b^* = 11.7$).

2.5.8. Water vapor permeability (WVP)

The WVP test was performed gravimetrically in triplicate following the ISO 53097:2002 standard. For this end, circular films (10 cm^2) were placed and sealed on permeability cups from TQC Sheen B.V. model VF2200 (Capelle aan den IJssel, Netherlands). Two grams of dried silica gel (0% RH) was placed in each cup and subsequently sealed with the films and placed in a desiccator with a saturated KNO_3 solution at a RH of approximately 80% and at 25 ± 1 °C. Finally, each cup was weighed hourly for a total of 6 h. The variation of cup weight was plotted as a function of time and the slope was obtained by linear regression, to calculate the water vapor transmission rate (WVTR) by the following Equation (4):

$$\mathrm{WVTR} = \frac{\Delta m}{t \times A} \quad (4)$$

where Δm is the weight gain of the cup (kg) at time t (s) and A is the

Table 1
Composition and coding FBP films with different amounts of PL.

Code	Content			
	Proteins (g)	Glycerol (g)	Water (g)	PL (wt% on dry FBP)
FBP	3	0.9	96.1	0
FBP/PL-2.5%	3	0.9	96.1	2.5
FBP/PL-5.0%	3	0.9	96.1	5.0
FBP/PL-7.5%	3	0.9	96.1	7.5
FBP/PL-10%	3	0.9	96.1	10.0

exposed area of the film (m^2).

On the other hand, the water vapor permeability (WVP) was calculated according to the following Equation (5):

$$WVP = \frac{WVTR}{S \times (RH_1 - RH_2)} \times e \quad (5)$$

where S is saturation pressure of water vapor at test temperature (Pa), RH_1 is the relative humidity inside of the desiccator (%) and RH_2 is the relative humidity inside the cup (%) and e is the average thickness of sample (mm).

2.5.9. Field emission scanning electron microscopy (FESEM)

A FESEM model ZEISS ULTRA55 Oxford Instruments (Abingdon, UK) was used to analyze the morphology of the cryofractured surfaces of the different films. Prior to observation, the samples were metallized with a gold-palladium alloy in a sputter coater EMITECH mod. SC7620 Quorum Technologies Ltd., (East Sussex, UK). Samples were analyzed at an accelerating voltage of 2 kV.

2.5.10. Attenuated total reflection-fourier transform infrared spectroscopy (ATR-FTIR)

The FTIR curves for the FBP films were obtained using an infrared spectrometer with an attenuated total reflection accessory (ATR) from PerkinElmer (Massachusetts, USA). Each sample was subjected to a total of 16 scans in 4000 and 500 cm^{-1} range using a resolution of 4 cm^{-1}. The obtained spectra were baseline corrected and normalized to a limiting ordinate of 1 absorbance unit.

2.5.11. Statistical analysis

Statistical analysis was performed to establish the effect of lignin content on the mechanical, optical and water susceptibility properties of the different obtained films. Analysis of variance (ANOVA) was performed on the experimental data and mean values were compared at a 95% confidence level ($p < 0.05$) according to Tukey's test using OriginPro2018 software.

3. Results and discussion

3.1. Thermal properties

The effect of PL content on the thermal stability of the FBP films was studied by thermogravimetric analysis (TGA). Fig. 1 shows the TGA and the first derivative curves (DTG) plots of lignin, FBP film and FBP/PL films. The main degradation temperatures of the films are summarized in Table 2. It can be seen that FBP film and its composites with PL show three degradation stages (Rojas-Lema et al., 2021). The first degradation stage is related to the evaporation of moisture contained in the films. In this first stage, the addition of lignin in the FBP film hardly has an effect on the moisture evaporation temperature, except for the sample reinforced with 10% lignin, where there is a significant increase in the degradation temperature, changing from 105.8 °C for the unreinforced FBP film up to 121.4 °C for the film reinforced with 10% PL. This increase in temperature in the first stage of the film reinforced with 10% PL may be due to the good dispersion of the lignin particles in the protein matrix, which act as a barrier effect hindering the water vapor evaporation (Yang et al., 2015). The second degradation stage involves the degradation of the glycerol used as plasticizer. In this case, it can be observed that the addition of lignin in the FBP film leads to a slight increase in the degradation temperature, obtaining a degradation temperature of around 242 °C for all the reinforced FBP films regardless the PL content. The higher degradation temperature may also be the result of the barrier effect caused by the good dispersion of the lignin particles in the film, which delays the degradation of the glycerol (Gomide et al., 2021). Finally, the third degradation process is associated with the protein degradation, which takes place at around 295.5 °C. After the addition of different amounts of PL to the FBP films, the final degradation temperature increases as the lignin amount in the FBP matrix rises, reaching the highest degradation temperature in the sample with 10% PL, 309.3 °C. This increase in protein degradation temperature can be due to the higher thermal stability of lignin with respect to proteins, and

Table 2
Thermal degradation temperatures and residue mass of pine cone lignin (PL) and FBP films reinforced with different amounts of PL obtained by thermogravimetry (TGA).

Sample	T_0[a] (°C)	T_{max} Stage 1 (°C)	T_{max} Stage 2 (°C)	T_{max} Stage 3 (°C)	Residue Mass (%)
PL	48.9 ± 0.9[a]	–	253.4 ± 2.3[a]	377.9 ± 2.1[a]	36.4 ± 1.1[a]
FBP	61.9 ± 1.5[b]	105.8 ± 2.5[a]	236.3 ± 2.0[b]	295.5 ± 1.9[b]	20.5 ± 0.2[b]
FBP/PL-2.5%	56.4 ± 2.3[c]	101.1 ± 2.0[a]	244.4 ± 1.2[b]	298.4 ± 1.4[b]	20.6 ± 0.4[b]
FBP/PL-5.0%	55.5 ± 1.6[c]	103.1 ± 3.1[a]	241.5 ± 0.5[b]	301.3 ± 2.1[b]	21.2 ± 0.3[b]
FBP/PL-7.5%	65.8 ± 1.5[d]	101.3 ± 1.8[a]	240.8 ± 1.3[b]	304.7 ± 1.2[b]	24.2 ± 0.3[c]
FBP/PL-10%	88.4 ± 4.9[e]	121.4 ± 3.7[b]	242.4 ± 2.1[b]	309.3 ± 1.7[b]	25.6 ± 0.5[d]

[a]T_0 was calculated with a weight loss of 1%.
[a] Different letters in the same column indicate a significant difference ($p < 0.05$).

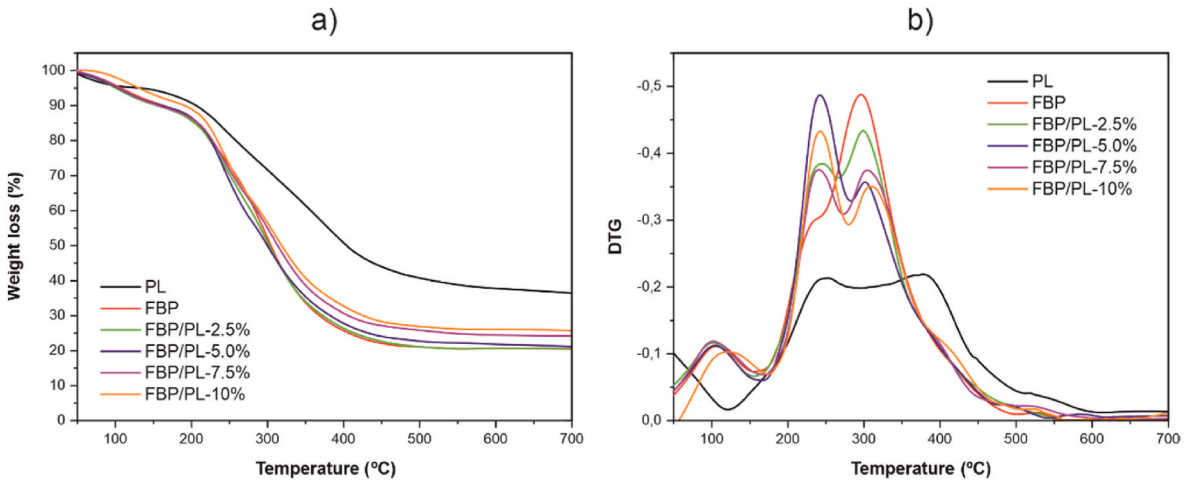

Fig. 1. Thermogravimetric (a) and first TG derivative (b) plots of lignin and FBP films reinforced with different amounts of PL.

also to the interactions between proteins and lignin, that lead to an improvement in the overall thermal stability compared to the control FBP film (Zadeh et al., 2018). As it has been reported by Oliveiro et al. (Oliviero et al., 2011), hydrogen bonding interactions between amino acid groups in zein protein and lignin functional groups have a positive effect on thermal stability. As they confirmed in zein-lignin nanocomposites, these interactions are more intense at low lignin concentrations. The strong hydrogen bonding is responsible for destructuring secondary structures of the zein protein which allowed an extensive protein conformational change with a positive effect on overall properties, including mechanical and thermal behaviour.

With regard to lignin, as can be seen, its degradation occurs slowly over a wide temperature range. Several authors have shown that its degradation extends to temperatures higher than 900 °C (Haykiri-Acma et al., 2010; Sameni et al., 2014). This wide range of lignin degradation is due to the structural complexity of this molecule, which is formed by a multitude of aromatic rings with high branching. The higher thermal stability of lignin, together with fixed carbon and mineral matter formed during its pyrolysis is the reason why the residue observed at 700 °C in the films increases as the lignin content in FBP films increases (Wądrzyk et al., 2021).

3.2. Mechanical properties

The thickness and tensile mechanical properties of FBP film and FBP/PL films are shown in Table 3. Results show that, the control film (FBP) has a tensile strength around 4.9 MPa, a Young's modulus close to 182 MPa and an elongation at break of 54%. The addition of PL to the FBP film results in higher tensile strength, with the tensile strength increasing as the PL content in the film rises. As can be seen, the FBP film reinforced with 10% PL has the highest tensile strength, with a value of 9.3 MPa, which represents an increase of around 90% with respect to the values obtained for the unreinforced FBP film. This increase in tensile strength may be due to the good compatibility between proteins, glycerol and lignin, since the hydroxyl groups (–OH) contained in FBP and glycerol are able to bind to the hydrophilic groups present in PL, creating strong linkages between the matrix and the reinforcement (Gomide et al., 2021). On the other hand, it can be observed that the Young's modulus also increases as the PL content in the FBP films increases, except in the film with a 5% of PL content, where a decrease is observed with respect to the film reinforced with 2.5% PL. In this case, the film with the highest stiffness is the FBP film containing 10% PL, with a Young's modulus value of 378.2 MPa, representing a 108% increase over the control film. As with tensile strength, the increase in Young's modulus in PL-reinforced films may be due to strong intramolecular and intermolecular interactions between proteins and lignin that restrict segment rotation and molecular mobility, thus increasing the resistant mechanical properties (Huang et al., 2003).

Table 3
Thickness and tensile properties of FBP films reinforced with different amounts of PL.

Sample	Thickness (μm)	Tensile Strength (MPa)	Young's Modulus (MPa)	Elongation at break (%)
FBP	292.5 ± 12.5[a]	4.9 ± 0.2[a]	182.4 ± 17.2[a]	54.0 ± 3.5[a]
FBP/PL-2.5%	258.7 ± 11.8[b]	4.8 ± 0.5[a]	239.4 ± 12.5[b]	60.5 ± 5.9[b]
FBP/PL-5.0%	351.2 ± 33.7[c]	5.3 ± 0.8[b]	196.2 ± 8.6[c]	111.7 ± 7.7[c]
FBP/PL-7.5%	297.5 ± 17.1[d]	5.5 ± 0.4[c]	243.5 ± 9.2[d]	99.9 ± 1.9[d]
FBP/PL-10%	372.5 ± 23.3[e]	9.3 ± 0.3[d]	378.2 ± 5.2[e]	56.4 ± 4.9[e]

[a] Different letters in each property indicate statistically significant differences between samples ($p < 0.05$).

As shown in Table 3, the incorporation of PL to the FBP film leads to an increase in the elongation at break for all samples, except for the film reinforced with 10% PL, which has an elongation at break similar to the control film. As can be seen, the sample reinforced with 5% PL has the highest elongation at break with a value of 111.7%, which represents an increase of around 107% compared to the control film. For PL contents higher than 5%, a decrease in elongation at break is observed. This increase in the elongation at break of reinforced samples with a lignin content lower than 10% may be due to the molecular weight variation of lignin, since the low molecular weight fraction can lead to a plasticizing effect, while the high molecular weight fraction leads to brittle materials, as demonstrated by Baumberger et al. (1998). Similar behavior was observed by J Huang et al. (2003) after addition of different amounts of alkaline lignin (AL) in soy protein isolate films. They reported that the incorporation of 10% AL in the soy protein film led to a simultaneous increase in tensile strength and elongation at break, whereas higher AL content led to a decrease in the elongation at break. Duval et al. (2013) also observed an increase in Young's modulus and a slight increase in elongation at break after addition of 15% kraft lignin in wheat gluten films. These unexpected properties in the films demonstrate the complexity of the interactions between proteins and lignin.

3.3. Water susceptibility

One of the main drawbacks of protein-based films is their high susceptibility to water due to their hydrophilic nature. Table 4 shows the water solubility, moisture content and contact angle values of FBP film and FBP/PL films. The results show that, the incorporation of PL to the FBP film leads to a decrease in moisture content. However, changes in moisture content are not statistically significant with increasing pine cone lignin content. Similar behaviour has been reported by Oliviero et al. in zein protein and different lignin content (Oliviero et al., 2011). They reported the control zein film had a water uptake of about 12% while the addition of lignin (lignosulfonate) in the 1–10 wt% range, did not provide a significant decrease in the water uptake due to the hydrophilic nature of the sulfonic acid groups. Anyway, they observed a slight decrease in water uptake of zein-lignin (lignosulfonate) nanocomposites up to 3 wt% lignin content. In contrast, they observed that the addition of alkaline lignin (AL) did provide a clear decrease in water uptake due to the hydrophobic nature of AL, specifically for a lignin content of 1 wt%. Thus, they confirmed that depending on the type of lignin, it can tailor the moisture absorption properties. In this work, the decrease in moisture content is not statistically significant which agrees with the results reported on zein-lignosulfonate nanocomposites. In this case, the slight reduction in moisture content in films reinforced with PL could also be due to the low availability of hydrophilic groups in the protein by the formation of intermolecular interactions via hydrogen bonds between this and lignin, resulting in a reduction of the number of active sites capable of interacting with water molecules (Sakunkittiyut

Table 4
Water solubility, moisture content and contact angle of FBP films reinforced with different amounts of PL.

Samples	Water solubility (%)	Moisture content (%)	Water contact angle (°)
FBP	31.1 ± 0.6[a]	15.5 ± 1.1[a]	57.3 ± 0.3[a]
FBP/PL-2.5%	30.2 ± 0.5[a]	15.3 ± 0.6[a]	56.5 ± 0.7[a]
FBP/PL-5.0%	30.0 ± 1.2[a]	14.9 ± 0.2[a]	45.9 ± 1.2[b]
FBP/PL-7.5%	30.4 ± 0.5[a]	13.7 ± 0.1[a]	43.6 ± 1.4[c]
FBP/PL-10%	29.9 ± 0.9[a]	13.7 ± 0.4[a]	40.9 ± 0.7[d]

[a] Different letters in each property indicate statistically significant differences between samples ($p < 0.05$).

et al., 2013; Yang et al., 2015). With regard to the water solubility of the FBP films, Table 4 shows that the addition of PL into the FBP films hardly affects it, obtaining for all the PL-reinforced FBP films similar water solubility values to that of the control FBP film, around 30%. The surface hydrophilicity of the FBP films was also confirmed by measuring the water contact angle on the film side exposed to air during films drying. As shown in Table 4, the water contact angle of the control FBP film is 57.3°. After the addition of PL into it, the water contact angle decreases with increasing PL content. It can be seen that the lowest contact angle was obtained in the film with the highest lignin content (10%), in which a water contact angle of 40.9° was obtained, representing a decrease of about 29% with respect to the control FBP film. Although this result can be contradictory, this behavior is due to the increase in surface roughness caused by the presence of lignin in the film, which favors wetting and could mask the hydrophobic effect of lignin observed in the moisture content (Crouvisier-Urion et al., 2016).

3.4. Structural chemical properties

Fig. 2 shows FTIR-ATR spectra of the control FBP film and the FBP films reinforced with PL in the wavenumber range comprised between 4000 and 500 cm^{-1}. First, the control film exhibits characteristic bands between 500 and 750 cm^{-1}, which correspond to the glycerol plasticizer (Gomide et al., 2021). These bands can be observed in all the spectra shown in Fig. 2. Other main peaks are observed at 900 and 1150 cm^{-1}, ascribed to the N–H bond and C–H stretching vibration (type III amide). The bands between 1400 and 1550 cm^{-1} are related to the type II amide N–H stretching, while peaks between 1600 and 1700 cm^{-1} are related to the C═O and C–N stretching vibration of the type I amide (Carvalho et al., 2020). It can be observed a decrease in these last peaks with an increase in lignin concentration. This effect is especially noticeable in the FBP/PL-7.5% film. A similar phenomenon was registered by Alvarenga et al. (Gomide et al., 2021), who related this decrease in the intensity of the peaks to the presence of secondary proteins that lose their conformation during the heating of the solutions that would form the film, provoking different interactions between the elements in the solution that, as a result, decrease the intensity of the main bands of the control FBP film. Another reason for this observation could be the dilution effect of faba bean proteins, as they are partially substituted by lignin. The peaks at 2850 and 2980 cm^{-1} are ascribed to the stretching of the C–H group, and the peak at 3272 cm^{-1} is associated with the O–H and N–H groups contained in the faba bean protein (Ramos et al., 2013). The addition of lignin to FBP did not provoke significant changes in the FTIR spectra, but only the protein dilution effect aforementioned and some changes in the intensity of the type III amide characteristic peaks, which could be an indicator of certain interaction between polypeptide chains in the proteins and lignin.

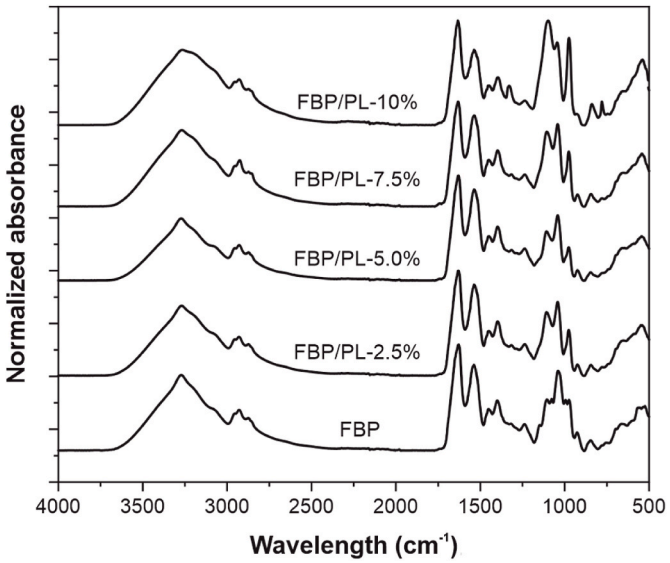

Fig. 2. FTIR spectra of FBP films reinforced with different amounts PL.

3.5. Morphological properties

Fig. 3 shows the cryofractured cross-sections of the different films obtained by FESEM. First, FBP control film (Fig. 3a) is seen to have a homogeneous and smooth surface with some porosity in it. This morphology matches the results observed in a previous study (Rojas-Lema et al., 2021). The addition of PL changes the microstructure of the FBP films, making more pores and microcracks to appear all over the surface. The concentration and size of the pores seems to increase with the lignin content. A similar surface modification was observed by Yang et al. (Yang et al., 2015) in wheat gluten films containing lignin nanoparticles. This is especially noticeable in the 7.5 and 10% PL samples (Fig. 3d and e), which could be related to an excessive amount of lignin particles in the films, resulting in the formation of agglomerates. This increase in the number and size of pores as the lignin content increases can negatively affect the mechanical and barrier properties of the films. It has been observed that lignin reinforced FBP films with contents higher than 5% PL led to a decrease in ductile mechanical properties, lower elongation at break, and higher water permeability.

3.6. Water vapor barrier properties

To evaluate the barrier properties of the films, the water vapor permeability (WVP) was studied, as they are a limitation for protein films, which are highly hydrophilic. Fig. 4 gathers the WVP results for the FBP control film and the FBP films with PL. As can be seen, the FBP film showed a WVP of approximately $3.02 \cdot 10^{-15}$ kg m/m^2·s·Pa. The addition of 2.5% of lignin positively affected WVP, reducing it down to $2.27 \cdot 10^{-15}$ kg m/m^2·s·Pa respectively, which is a reduction of permeability 24.7% to the control film. This means that barrier properties against water vapor improved in the films thanks to the incorporation of PL. This reduction could be ascribed to a good dispersion of lignin in the FBP polymeric matrix, obstructing water vapor diffusion and increasing the length of the flow path through the films (Dias et al., 2019). Moreover, the hydrophobicity of lignin may have supported this effect by reducing the affinity of the film towards water molecules (Duval et al., 2013). On the other hand, the addition of moderate lignin contents in the FBP film, 5% and 7.5% PL, did not have a substantial influence on the WVP, with very similar values to those recorded in the control film. In the sample reinforced with 10% PL, it is noted that the WVP increases compared to the unreinforced film, obtaining a value of $3.39 \cdot 10^{-15}$ kg m/m^2·s·Pa, which represents an increase of about 13%. This fact could be related to an excess of lignin particles in the film, which may have formed agglomerates that provoked the formation of less cohesive film, making water vapor diffusion easier. A similar behavior was observed by Alvarenga et al. (Gomide et al., 2021). These results agree with the findings observed in FESEM images, where sample with 10% of PL showed higher concentration of holes and pores in the microstructure, which would clearly increase water vapor permeability and decrease barrier properties.

3.7. Optical properties

Visual appearance of the films is an essential aspect regarding their use in the food packaging industry, as this may affect how the customer perceive the product. At first glance, the control film is the only one that offers some transparency, while the rest of the films exhibit a strong dark color, as a result of the incorporation of lignin. The visual appearance of the control film is very similar to the one shown in previous studies (Rojas-Lema et al., 2021).

Table 5 gathers the main color parameters of the developed films in

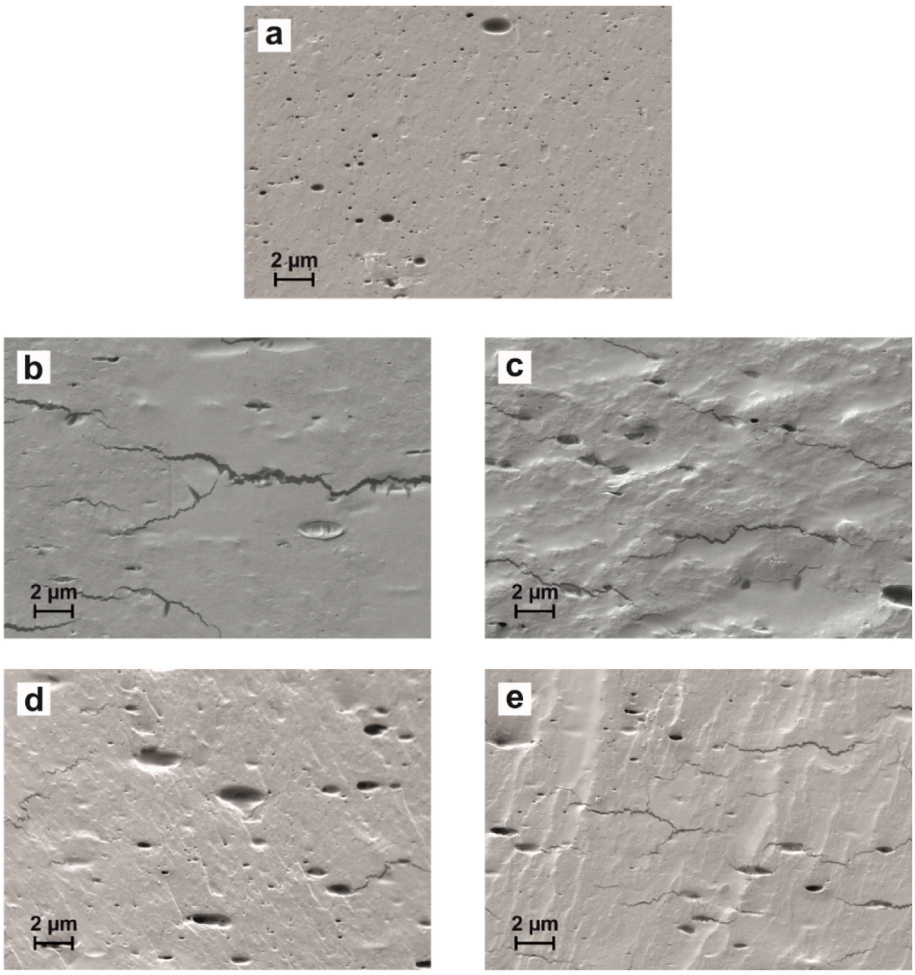

Fig. 3. Images at 5000 × of cryofractured cross-section obtained by FESEM of the samples of (a) FBP; (b) FBP/PL-2.5%; (c) FBP/PL-5.0%; (d) FBP/PL-7.5%, and (e) FBP/PL-10%.

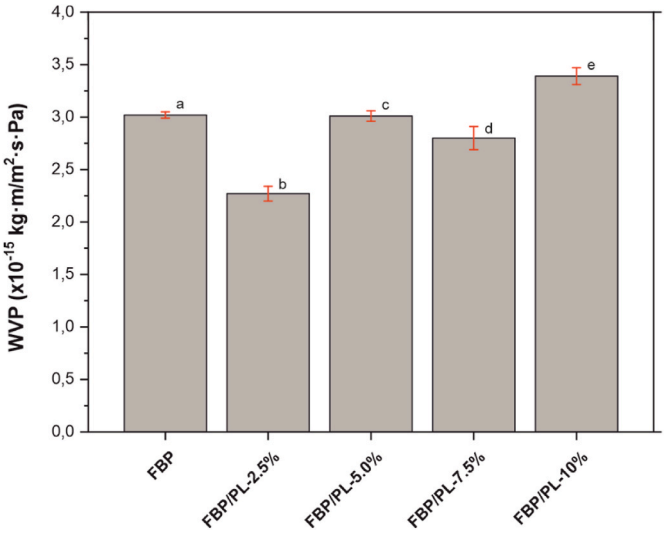

Fig. 4. Water vapor permeability (WVP) of FBP films reinforced with different amounts of PL.

terms of the color coordinates of the chromatic space CIELab. L^* is representative for the lightness. As expected, the control FBP film with the most translucent appearance were measured to be the lightest (L* 40.9). Incorporation of PL to the films reduced the measured L* to

Table 5
Optical parameters of FBP films reinforced with different amounts of PL.

Code	L^*	a^*	b^*	ΔE (Control)[a]
FBP	41.0 ± 0.3[a]	1.7 ± 0.2[a]	11.7 ± 0.[aa]	–
FBP/PL-[a].5%	25.7 ± 0.1[b]	0.9 ± 0.3[b]	0.9 ± 0.1[b]	18.7 ± 0.0[a]
FBP/PL-5.[a]%	25.1 ± 0.0[b]	0.6 ± 0.1[c]	0.3 ± 0.1[c]	19.5 ± 0.1[a]
FBP/PL-7.[a]%	25.0 ± 0.1[b]	0.5 ± 0.1[d]	0.6 ± 0.1[d]	19.4 ± 0.1[a]
FBP/PL-10[a]	25.0 ± 0.2[b]	0.2 ± 0.1[e]	0.6 ± 0.3[d]	19.5 ± 0.1[a]

[a] ΔE is[a]obtained from the color difference between the FBP film and every FBP/PL film.
[a] Different letters in each property indicate statistically significant differences between samples ($p < 0.05$).

approximately 25 indicating that the films became darker (Weatherall and Coombs, 1992). It should be noted that all the parameters of the FBP/PL films are very similar between them, as their color is almost the same. Color coordinate a^* stands for green (negative) and red (positive), so all the films have positive values due to presenting brown tonalities. Additionally, a^* appears to decrease as the PL content increases, this is probably attributed to an increase in the darkness of the color with the PL content. Similarly, color coordinate b^*, which represents the change from blue (negative) to yellow (positive), exhibits positive values, which was also expected due to the films having certain yellowness, especially the control FBP film. Furthermore, b^* also decreases when PL is incorporated into the films, due to approaching to darker colors. Finally, as a consequence of the very similar color between all the FBP/PL films, the

ΔE parameter is practically invariable, as it indicates the difference in color compared to the FBP control film.

4. Conclusions

The present work studies the effect of the incorporation of different amounts of lignin extracted from pine cone (2.5, 5.0, 7.5 and 10 wt%) on the thermal, mechanical, morphological, water susceptibility, chemical, barrier and optical properties of glycerol-plasticized faba bean protein films. The addition of lignin in the protein film increased its ductile mechanical properties due to the plasticization effect of the low molecular weight fraction present in the lignin. In this case, an increase in the elongation at break of the lignin-reinforced films was observed, being the film reinforced with 5% the one with the highest elongation at break, 111.7%, representing an increase of 107% compared to the control film. Higher lignin contents (7.5 and 10%) led to a decrease in the elongation at break due to the formation of aggregates that promote the formation of pores and microcracks in its internal structure as could be observed in the FESEM images. Regarding the mechanical strength properties, it was observed that the addition of lignin led to an increase in tensile strength, resulting in a higher increase as the lignin content increases. The thermal stability of the FBP film was also affected by the presence of lignin. In this case, the incorporation of lignin resulted in an increase in the thermal stability of the FBP film, increasing the characteristic degradation temperatures of glycerol and proteins. This increase in thermal stability was more evident in the 10% PL reinforced film and this was attributed to several factors such as the good dispersion of lignin in the FBP polymeric matrix which hinders the degradation of other components, the higher thermal stability of lignin and the formation of intramolecular interactions between lignin and proteins, which have been analyzed by FTIR. On the other hand, as it was stated in the hypotheses of the work, the linkages formed between the lignin and the protein, mainly through hydrogen bonds, led to a reduction in the number of active sites in the protein that are able to interact with water molecules. This phenomenon, together with the inherent hydrophobicity of lignin, led to an increase in the hydrophobicity of the lignin-reinforced FBP films, which was manifested by a decrease in moisture content. In this case, it was observed that films with a higher lignin content of 7.5 and 10% PL, showed the greatest reduction in moisture content, decreasing it by about 12% compared to the control FBP film. The addition of lignin to the FBP film also resulted in an improvement of the barrier properties, with a noticeable reduction in WVP compared to the control FBP film. As can be seen, the film with 2.5% PL is the film with the lowest WVP value, which means a reduction of around 25% with respect to the control FBP film. In addition, it was possible to observe how the addition of lignin had a remarkable influence on the colour and opacity of the films, obtaining completely opaque and dark films. This study has demonstrated how lignin derived from pine cone could be an interesting functional additive to improve the thermal, barrier, mechanical and water susceptibility properties of faba bean protein films, allowing to obtain bio-based films that offer a high potential to be considered for their use in the packaging applications.

Author statement

Sandra Rojas-Lema: Data curation, Software, Formal analysis, Writing – original draft, Klara Nilsson: Investigation, Validation, Data curation, Maud Langton: Resources, Project administration, Funding acquisition, Jon Trifol: Investigation, Validation, Data curation, Jaume Gomez-Caturla: Data curation, Software, Formal analysis, Writing – original draft, Rafael Balart: Conceptualization, Supervision, Project administration, Funding acquisition, Daniel Garcia-Garcia: Methodology, Investigation, Validation, Writing – review & editing, Visualization, Rosana Moriana: Conceptualization, Supervision, Project administration

Declaration of competing interest

The authors declare that they have no known competing financial interests or personal relationships that could have appeared to influence the work reported in this paper.

Data availability

Data will be made available on request.

Acknowledgements

This research is a part of the grant PID2020-116496RB-C22 funded by MCIN/AEI/10.13039/501100011033, and the projects AICO/2021/025 and CIGE/2021/094 funded by Generalitat Valenciana-GVA. Funding for open access charge: Universitat Politècnica de València. S. Rojas-Lema thanks the Generalitat Valenciana-GVA for the financial support through a Santiago Grisolia grant (GRISOLIAP/2019/132). J. Gomez-Caturla wants to thank Generalitat Valenciana-GVA, for his FPI grant (ACIF/2021/185) and grant FPU20/01732 funded by MCIN/AEI/10.13039/501100011033 and by ESF Investing in your future. D. Garcia-Garcia wants to thank the Ministry of Science, Innovation and Universities for their financial support through the "José Castillejo" mobility grant (CAS19/00332). Microscopy services at UPV are acknowledged for their help in using and collecting FESEM images. J. Trifol also acknowledges the financial support of Academy of Finland's Flagship Programme under Projects No. 318890 and 318891 (Competence Center for Materials Bioeconomy, FinnCERES).

References

Agarwal, S., 2021. Major factors affecting the characteristics of starch based biopolymer films. Eur. Polym. J. 160, 110788.
Alharbi, N.H., Adhikari, K.N., 2020. Factors of yield determination in faba bean (Vicia faba). Crop Pasture Sci. 71 (4), 305–321.
Anker, M., Stading, M., Hermansson, A.-M., 2000. Relationship between the microstructure and the mechanical and barrier properties of whey protein films. J. Agric. Food Chem. 48 (9), 3806–3816.
Arancibia, M.Y., López-Caballero, M.E., Gómez-Guillén, M.C., Montero, P., 2014. Release of volatile compounds and biodegradability of active soy protein lignin blend films with added citronella essential oil. Food Control 44, 7–15.
Austin, A.T., Ballaré, C.L., 2010. Dual role of lignin in plant litter decomposition in terrestrial ecosystems. Proc. Natl. Acad. Sci. USA 107 (10), 4618–4622.
Baumberger, S., Lapierre, C., Monties, B., 1998. Utilization of pine kraft lignin in starch composites: impact of structural heterogeneity. J. Agric. Food Chem. 46 (6), 2234–2240.
Bourtoom, T., 2009. Edible protein films: properties enhancement. International Food Research Journal 16 (1), 1–9.
Carvalho, R.A., de Oliveira, A.C.S., Santos, T.A., Dias, M.V., Yoshida, M.I., Borges, S.V., 2020. WPI and cellulose nanofibres bio-nanocomposites: effect of thyme essential oil on the morphological, mechanical, barrier and optical properties. J. Polym. Environ. 28 (1), 231–241.
Ciobanu, C., Ungureanu, M., Ignat, L., Ungureanu, D., Popa, V., 2004. Properties of lignin–polyurethane films prepared by casting method. Ind. Crop. Prod. 20 (2), 231–241.
Crouvisier-Urion, K., Bodart, P.R., Winckler, P., Raya, J., Gougeon, R.D., Cayot, P., Domenek, S., Debeaufort, F., Karbowiak, T., 2016. Biobased composite films from chitosan and lignin: antioxidant activity related to structure and moisture. ACS Sustain. Chem. Eng. 4 (12), 6371–6381.
De Carvalho, R., Grosso, C., 2004. Characterization of gelatin based films modified with transglutaminase, glyoxal and formaldehyde. Food Hydrocolloids 18 (5), 717–726.
Denavi, G., Tapia-Blácido, D., Añón, M., Sobral, P., Mauri, A., Menegalli, F., 2009. Effects of drying conditions on some physical properties of soy protein films. J. Food Eng. 90 (3), 341–349.
Dey, A., Dhumal, C.V., Sengupta, P., Kumar, A., Pramanik, N.K., Alam, T., 2021. Challenges and possible solutions to mitigate the problems of single-use plastics used for packaging food items: a review. J. Food Sci. Technol. 58 (9), 3251–3269.
Dias, M.V., Azevedo, V.M., Santos, T.A., Pola, C.C., Lara, B.R.B., Borges, S.V., Soares, N.F. F., Medeiros, É.A.A., Sarantópoulous, C., 2019. Effect of active films incorporated with montmorillonite clay and α-tocopherol: potential of nanoparticle migration and reduction of lipid oxidation in salmon. Packag. Technol. Sci. 32 (1), 39–47.
Duval, A., Molina-Boisseau, S., Chirat, C., 2013. Comparison of Kraft lignin and lignosulfonates addition to wheat gluten-based materials: mechanical and thermal properties. Ind. Crop. Prod. 49, 66–74.
Gadhave, R.V., Srivastava, S., Mahanwar, P.A., Gadekar, P.T., 2019. Lignin: renewable raw material for adhesive. Open J. Polym. Chem. 9 (2), 27–38.

Garcia, M.A., Martino, M.N., Zaritzky, N.E., 2000. Lipid addition to improve barrier properties of edible starch-based films and coatings. J. Food Sci. 65 (6), 941–944.
Gnanasekaran, D., 2019. Green Biopolymers and Their Nanocomposites. Springer.
Gomide, R.A.C., de Oliveira, A.C.S., Luvizaro, L.B., Yoshida, M.I., de Oliveira, C.R., Borges, S.V., 2021. Biopolymeric films based on whey protein isolate/lignin microparticles for waste recovery. J. Food Process. Eng. 44 (1), e13596.
González, A., Gastelú, G., Barrera, G.N., Ribotta, P.D., Igarzabal, C.I.Á., 2019. Preparation and characterization of soy protein films reinforced with cellulose nanofibers obtained from soybean by-products. Food Hydrocolloids 89, 758–764.
González, A., Strumia, M.C., Igarzabal, C.I.A., 2011. Cross-linked soy protein as material for biodegradable films: synthesis, characterization and biodegradation. J. Food Eng. 106 (4), 331–338.
Haykiri-Acma, H., Yaman, S., Kucukbayrak, S., 2010. Comparison of the thermal reactivities of isolated lignin and holocellulose during pyrolysis. Fuel Process. Technol. 91 (7), 759–764.
Hendawey, M., Younes, A., 2013. Biochemical evaluation of some faba bean cultivars under rainfed conditions at El-Sheikh Zuwayid. Ann. Agric. Sci. (Cairo) 58 (2), 183–193.
Huang, J., Zhang, L., Chen, P., 2003. Effects of lignin as a filler on properties of soy protein plastics. II. Alkaline lignin. J. Appl. Polym. Sci. 88 (14), 3291–3297.
Jongjareonrak, A., Benjakul, S., Visessanguan, W., Tanaka, M., 2006. Fatty acids and their sucrose esters affect the properties of fish skin gelatin-based film. Eur. Food Res. Technol. 222 (5), 650–657.
Khalil, H., Tye, Y., Saurabh, C., Leh, C., Lai, T., Chong, E., Fazita, M., Hafiidz, J.M., Banerjee, A., Syakir, M., 2017. Biodegradable polymer films from seaweed polysaccharides: a review on cellulose as a reinforcement material. Express Polym. Lett. 11 (4).
Kim, K.M., Hwang, K.T., Weller, C.L., Hanna, M.A., 2002. Preparation and characterization of soy protein isolate films modified with sorghum wax. J. Am. Oil Chem. Soc. 79 (6), 615–619.
Kokoszka, S., Debeaufort, F., Hambleton, A., Lenart, A., Voilley, A., 2010. Protein and glycerol contents affect physico-chemical properties of soy protein isolate-based edible films. Innovat. Food Sci. Emerg. Technol. 11 (3), 503–510.
Liu, C., Xiao, C., Liang, H., 2005. Properties and structure of PVP–lignin "blend films". J. Appl. Polym. Sci. 95 (6), 1405–1411.
Makishi, G., Lacerda, R., Bittante, A., Chambi, H., Costa, P., Gomide, C., Carvalho, R., Sobral, P., 2013. Films based on castor bean (Ricinus communis L.) proteins crosslinked with glutaraldehyde and glyoxal. Ind. Crop. Prod. 50, 375–382.
Marquié, C., 2001. Chemical reactions in cottonseed protein cross-linking by formaldehyde, glutaraldehyde, and glyoxal for the formation of protein films with enhanced mechanical properties. J. Agric. Food Chem. 49 (10), 4676–4681.
Masamba, K., Li, Y., Hategekimana, J., Liu, F., Ma, J., Zhong, F., 2016. Effect of Gallic acid on mechanical and water barrier properties of zein-oleic acid composite films. J. Food Sci. Technol. 53 (5), 2227–2235.
Montalvo-Paquini, C., Rangel-Marron, M., Palou, E., Lopez-Malo, A., 2013. Effect of pH on physical properties of edible films from faba bean protein. Recent Advances in Chemical Engineering, Biochemistry and Computational Chemistry 29–34.
Montalvo-Paquini, C., Rangel-Marrón, M., Palou, E., López-Malo, A., 2014. Physical and chemical properties of edible films from faba bean protein. Cellulose 8, 125–131.
Nagarajan, S., Radhakrishnan, S., Kalkura, S.N., Balme, S., Miele, P., Bechelany, M., 2019. Overview of protein-based biopolymers for biomedical application. Macromol. Chem. Phys. 220 (14), 1900126.
Niegelhell, K., Sußenbacher, M., Sattelkow, J.r., Plank, H., Wang, Y., Zhang, K., Spirk, S., 2017. How bound and free fatty acids in cellulose films impact nonspecific protein adsorption. Biomacromolecules 18 (12), 4224–4231.
Oliviero, M., Verdolotti, L., Di Maio, E., Aurilia, M., Iannace, S., 2011. Effect of supramolecular structures on thermoplastic Zein–Lignin bionanocomposites. J. Agric. Food Chem. 59 (18), 10062–10070.
Pagliaro, M., Ciriminna, R., Kimura, H., Rossi, M., Della Pina, C., 2007. From glycerol to value-added products. Angew. Chem. Int. Ed. 46 (24), 4434–4440.
Ramos, Ó.L., Reinas, I., Silva, S.I., Fernandes, J.C., Cerqueira, M.A., Pereira, R.N., Vicente, A.A., Poças, M.F., Pintado, M.E., Malcata, F.X., 2013. Effect of whey protein purity and glycerol content upon physical properties of edible films manufactured therefrom. Food Hydrocolloids 30 (1), 110–122.
Rhim, J.-W., 2004. Increase in water vapor barrier property of biopolymer-based edible films and coatings by compositing with lipid materials. Food Sci. Biotechnol. 13 (4), 528–535.
Rhim, J.W., Gennadios, A., Handa, A., Weller, C.L., Hanna, M.A., 2000. Solubility, tensile, and color properties of modified soy protein isolate films. J. Agric. Food Chem. 48 (10), 4937–4941.
Rojas-Lema, S., Nilsson, K., Trifol, J., Langton, M., Gomez-Caturla, J., Balart, R., Garcia-Garcia, D., Moriana, R., 2021. Faba bean protein films reinforced with cellulose nanocrystals as edible food packaging material. Food Hydrocolloids 121, 107019.
Sadasivuni, K.K., Saha, P., Adhikari, J., Deshmukh, K., Ahamed, M.B., Cabibihan, J.J., 2020. Recent advances in mechanical properties of biopolymer composites: a review. Polym. Compos. 41 (1), 32–59.
Sakunkittiyut, Y., Kunanopparat, T., Menut, P., Siriwattanayotin, S., 2013. Effect of kraft lignin on protein aggregation, functional, and rheological properties of fish protein-based material. J. Appl. Polym. Sci. 127 (3), 1703–1710.
Sameni, J., Krigstin, S., dos Santos Rosa, D., Leao, A., Sain, M., 2014. Thermal characteristics of lignin residue from industrial processes. Bioresources 9 (1), 725–737.
Saremnezhad, S., Azizi, M., Barzegar, M., Abbasi, S., Ahmadi, E., 2011. Properties of a new edible film made of faba bean protein isolate. J. Agric. Sci. Technol. 13 (2), 181–192.
Shankar, S., Reddy, J.P., Rhim, J.-W., 2015. Effect of lignin on water vapor barrier, mechanical, and structural properties of agar/lignin composite films. Int. J. Biol. Macromol. 81, 267–273.
Trifol, J., Marin Quintero, D.C., Moriana, R.J.A.S.C., 2021. Pine cone biorefinery: integral valorization of residual biomass into lignocellulose nanofibrils (LCNF)-reinforced composites for packaging 9 (5), 2180–2190. Engineering.
Upton, B.M., Kasko, A.M., 2016. Strategies for the conversion of lignin to high-value polymeric materials: review and perspective. Chem. Rev. 116 (4), 2275–2306.
Vioque, J., Alaiz, M., Girón-Calle, J., 2012. Nutritional and functional properties of Vicia faba protein isolates and related fractions. Food Chem. 132 (1), 67–72.
Wądrzyk, M., Janus, R., Lewandowski, M., Magdziarz, A., 2021. On mechanism of lignin decomposition–Investigation using microscale techniques: py-GC-MS, Py-FT-IR and TGA. Renew. Energy 177, 942–952.
Walker, T.R., McGuinty, E., Charlebois, S., Music, J., 2021. Single-use plastic packaging in the Canadian food industry: consumer behavior and perceptions. Humanities and Social Sciences Communications 8 (1), 1–11.
Weatherall, I.L., Coombs, B.D., 1992. Skin color measurements in terms of CIELAB color space values. J. Invest. Dermatol. 99 (4), 468–473.
Wolfson, A., Dlugy, C., Shotland, Y., 2007. Glycerol as a green solvent for high product yields and selectivities. Environ. Chem. Lett. 5 (2), 67–71.
Xia, S., Zhang, L., Davletshin, A., Li, Z., You, J., Tan, S., 2020. Application of polysaccharide biopolymer in petroleum recovery. Polymers 12 (9), 1860.
Yadav, A., Mangaraj, S., Singh, R., Kumar, N., Arora, S., 2018. Biopolymers as packaging material in food and allied industry. Int. J. Conserv. Sci. 6 (2), 2411–2418.
Yang, W., Kenny, J.M., Puglia, D.J.I.C., Products, 2015. Structure and properties of biodegradable wheat gluten bionanocomposites containing lignin nanoparticles. Ind. Crop. Prod. 74, 348–356.
Zadeh, E.M., O'Keefe, S.F., Kim, Y.-T., 2018. Utilization of lignin in biopolymeric packaging films. ACS Omega 3 (7), 7388–7398.